ADVANCED FUNCTIONAL MATERIALS

Light Out-Coupling Efficiencies of Organic Light-Emitting Diode Structures and the Effect of Photoluminescence Quantum Yield**

By *Lucy H. Smith*, *Jon A. E. Wasey*, *Ifor D. W. Samuel*, and *William L. Barnes**

Results obtained from modeling the light out-coupling efficiency of an organic light-emitting diode (OLED) structure containing the recently developed first-generation *fac*-tris(2-phenylpyridine) iridium-cored dendrimer (Ir-G1) as the emissive organic layer are reported. Comparison of the results obtained for this material with those of corresponding structures based upon small-molecule and polymer emissive materials is made. The calculations of out-coupling efficiency performed here take account of many factors, including the photoluminescence quantum yield (PLQY) of the emissive materials. Further, how each material system might perform with regard to out-coupling efficiency when a range of possible PLQYs are considered is shown. The calculations show that the very high efficiency of dendrimer-based OLEDs can be attributed primarily to their high PLQY.

1. Introduction

Organic light-emitting diodes (OLEDs) are now being fabricated from a number of different emissive materials,[1–6] with much work being done to improve the efficiency in each system. In addition, theoretical models have been developed to evaluate the optical performance of OLED designs,[7–9] both to understand their operation[10] and to allow improved devices to be designed.[11] The operation of an OLED involves charge injection and charge transport, the formation of excitons, and out-coupling of the light radiatively produced when the excitons decay. Light out-coupling is a very important aspect of OLED design; it is the area in which there is still the greatest scope for significant improvements in efficiency.

To date, many different methods have been used in an attempt to improve light out-coupling from OLEDs. In a conventional planar OLED, a large proportion of the emitted light is lost as guided modes. By introducing microstructure in one or more interfaces within an OLED, non-radiative guided modes such as surface plasmon–polariton (SPP) and waveguide modes can be coupled to radiation by scattering. There are a number of ways to do this. The use of a one-dimensional[12,13] or two-dimensional[14] periodic corrugation allows coupling to radiation via Bragg scattering. Random surface texturing of the top surface of an inorganic LED has been shown to permit partial extraction of waveguide-confined light via scattering,[15] and is a method which could be transferred to OLEDs. Similarly, arrays of hexagonally packed silica microspheres[16] and glass or plastic lens-shaped features[17] added to a substrate have led to increased light emission. Another contrasting method is the insertion of a low-refractive-index aerogel layer between the indium tin oxide (ITO) and glass substrate within a conventional OLED.[18]

In this paper, we model the optical out-coupling of planar OLEDs so as to compare the performance of three commonly used classes of material, and to investigate the extent to which the photoluminescence quantum yield (PLQY) affects the out-coupling. We explore the different routes by which excitons may lose their energy in the OLED structure, thus building up a picture of the different modes supported by the structure and their relative importance in determining the out-coupling efficiency.

There are three main classes of emissive organic semiconductors: small molecules, conjugated polymers, and conjugated dendrimers. Small-molecule emitters are deposited under vacuum conditions, whilst the conjugated materials may be spin-coated onto substrates. Dendrimers[19–21] are highly branched molecules, and conjugated dendrimers are very promising OLED materials.[5,6,22] They consist of a core, dendrons, and surface groups; this modular construction permits electronic properties and processing aspects to be optimized separately. The solubility of the dendrimer allows the use of a number of chromophores. We have modeled the out-coupling efficiency of devices based on three materials, the first-generation *fac*-tris(2-phenylpyridine) iridium-cored dendrimer (Ir-G1), the small molecule, aluminum tris-8-hydroxyquinoline (Alq_3), and the conjugated polymer, poly(2-methoxy-5-(2′-ethylhexyloxy)-1,4-phenylenevinylene) (MEH-PPV).

We also investigate the effect of the PLQY of the emissive materials. The external quantum efficiency (Φ_{ext}) of an OLED is given by:[23]

$$\Phi_{ext} = \Phi_c \Phi_s \Phi_{rad} \Phi_{esc} \quad (1)$$

where Φ_c is the efficiency with which electrons and holes combine to form excitons and Φ_s represents the fraction of excitons that is formed in a spin state capable of radiating (an emissive state); for phosphorescent materials this is unity, but for fluo-

[*] Prof. W. L. Barnes, L. H. Smith, Dr. J. A. E. Wasey
School of Physics, University of Exeter
Exeter EX4 4QL (UK)
E-mail: l.h.smith@ex.ac.uk
Prof. I. D. W. Samuel
Organic Semiconductor Centre, School of Physics and Astronomy
University of St. Andrews
North Haugh, St. Andrews, Fife KY16 9SS (UK)

[**] The authors thank both the EPSRC (through the DTI-LINK project XTRAOLED) and CDT Ltd. for financial support.

 DOI: 10.1002/adfm.200500283

rescent materials only excitons in the singlet spin state are able to decay. Of the emissive-state excitons produced, only a fraction, Φ_{rad}, will decay radiatively and generate light inside the OLED, of which a fraction, Φ_{esc}, will be out-coupled as photons that leave the structure. Φ_{rad} is the fraction of potentially emissive excitons produced which decay radiatively; here we take this to be equal to the PLQY; it is the effect of this efficiency that we investigate here. In the first part of the paper, we assume a PLQY of 100 %; in the second part the effect of a lower PLQY is examined.

2. Methods

We consider the simple OLED structure illustrated in Figure 1. It consists of an optically thick aluminum cathode, the organic layer under investigation, a 100 nm thick ITO anode, and, finally, a thick silica substrate through which the light is emitted. Although aluminum on its own is not an electrically

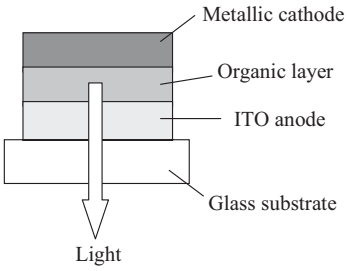

Figure 1. The OLED structure studied. Electrons and holes injected from the cathode and anode, respectively, combine to form excitons, which subsequently decay to produce light.

efficient cathode, the addition of a very thin layer of LiF between the aluminum and organic layers greatly improves its electron-injection efficiency.[24] Calculations (not shown) indicate that the optical effect of such a thin LiF layer is negligible so that here, for the purposes of optical modeling, we ignore it. The organic layer contains the light emitters and is either the dendrimer, the small molecule emitter Alq_3, or the conjugated polymer, MEH–PPV. In each case, we have calculated the optimum organic layer thickness required to give maximum radiation from the structure. These optimized thicknesses are 145, 130, and 110 nm for the dendrimer, Alq_3, and MEH–PPV systems, respectively. Although it is common to have several organic layers in an OLED, these are often of similar refractive index. Here, we have assumed that they can be represented as one layer with the excitons located within this layer so as to optimize the optical out-coupling. From this point on, the results discussed refer to these optimized structures. It should be noted that, in altering the layer thicknesses to optimize optical performance, a real device will also need to be optimized with regard to electrical efficiency. Optimizing both may require a compromise to be made, something that we have not considered here.

The optical properties of both Alq_3 and MEH–PPV have been relatively well determined.[12] One of the key differences between these two materials is the fact that the emitters, or more specifically, the dipole moments associated with radiating excitons, have different orientations. The dipole moments in Alq_3 are effectively isotropic, sampling all directions in space on a time scale much shorter than the fluorescence lifetime.[25] In contrast, the dipole moments in the polymer lie within the plane of the layer.[26] The peak emission of Alq_3 occurs at 550 nm, and that of MEH–PPV at 580 nm. Another difference between Alq_3 and the polymer is that the latter is birefringent; the effects of this birefringence are accounted for within the model used here.

The dendrimer organic layer modeled here is based on the light-emissive Ir-G1 contained within a host material 4,4′-bis(*N*-carbazole) biphenyl (CBP). It has been shown experimentally[6] that the use of this host material significantly enhances the efficiency of the device. Here we model a 20:80 wt.-% blend of the dendrimer and CBP. The peak emission wavelength of this organic layer occurs at 518 nm. Measurements conducted in our laboratories (not shown) indicate this material has little or no birefringence. The optical parameters we have used are given in the Appendix.

We make use of a specially adapted classical technique to calculate the power lost by an emissive dipole in a multilayered structure.[7,8] The model allows both identification of the modes in a given structure, and calculation of the strength of the coupling between the emitter and these modes. The emitters are considered to be forced, damped, electric-dipole oscillators. The dipole field is represented by a sum of plane waves; each plane wave is characterized by a different in-plane wavevector, k_x, where k_x is the component of the wavevector parallel to the interfaces.

By calculating the power dissipated by the dipole as a function of the in-plane wavevector, we are able to produce a power-dissipation spectrum. When the in-plane wavevector of the dipole emission matches that of a mode of the structure, the dipole may resonantly lose power to that mode. Thus, peaks in the power-dissipation spectrum indicate the different modes of the structure. A power-dissipation spectrum for the dendrimer-based structure is shown in Figure 2a for an emission wavelength of 518 nm. By calculating the power dissipated as a function of both frequency and in-plane wavevector, we can build up a dispersion diagram of the modes of the system, as shown in Figure 2b. The dark features correspond to coupling between the emitter and the optical modes of the structure. This particular plot is for an emissive layer in which we assume the light is generated in the middle of the organic layer. The dipole layer is considered to be infinitely thin. Dissipated power with an in-plane wavevector $k_x < n_{silica} k_0$, where k_0 is the wavevector of a photon in free space and n_{silica} is the refractive index of silica, corresponds to light that may propagate in the thick silica substrate. Of this power, the fraction with in-plane wavevectors less than k_0 relates to light that may leave the structure and produce useful far-field radiation, though a small amount will be lost to absorption in the OLED materials. Our model allows us to calculate how much power is radiated

ADVANCED FUNCTIONAL MATERIALS

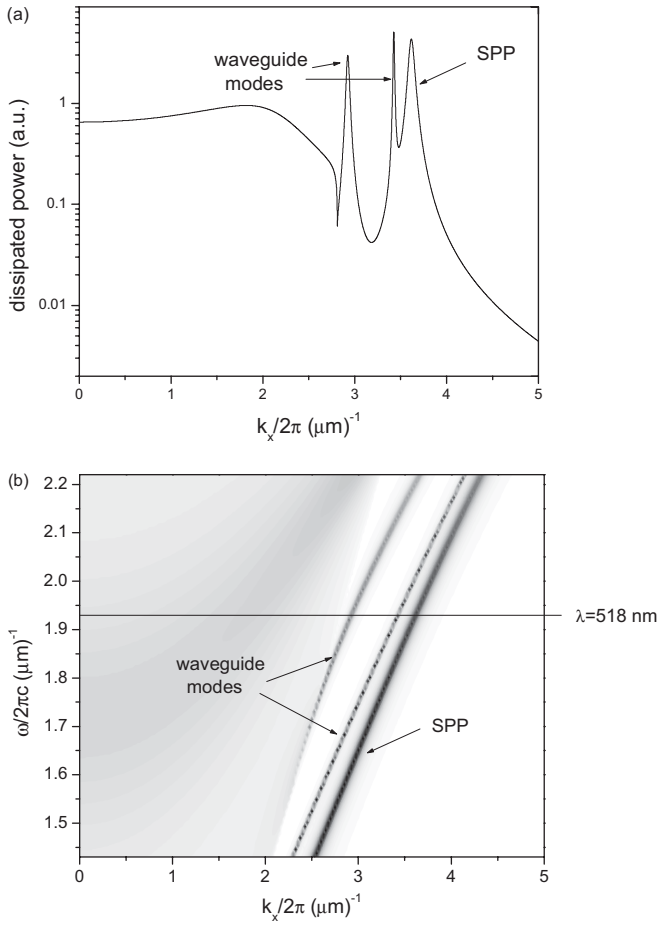

Figure 2. a) The power-dissipation plot for a single emission wavelength of 518 nm, and b) the dispersion diagram formed by calculating the dissipated power as a function of frequency (ω) and in-plane wavevector; the nature of the different modes is indicated.

out through the substrate, as well as how much is lost to the waveguide, SPP, and substrate modes; it also allows us to calculate how much power is quenched directly by the absorptive cathode and anode.[27] It should be noted that quenching due to charge carriers within the organic layer is not included in the model. The features labeled at higher in-plane wavevectors correspond to optical modes that cannot propagate in the substrate or in free space; they are modes that are trapped within the structure. For the particular structure modeled here, there are two waveguide modes and one surface plasmon–polariton mode. Surface plasmon–polaritons result from the coupling between the free charges at the surface of a metal and electromagnetic (EM) radiation.[28] This leads to longitudinal surface-charge density fluctuations that propagate along the interface, and an associated oscillating EM field that decays exponentially with distance from the metal surface. For the structure considered here, the SPP mode occurs at the metal/dielectric interface formed by the boundary between the aluminum cathode and the organic layer.

To determine the amount of power coupled to a specific mode, the area under the relevant peak in the power-dissipation spectrum (Fig. 2a) was integrated. By normalizing these power values to the total amount of power dissipated by the dipole, we obtain the fraction of the emitted power that is lost

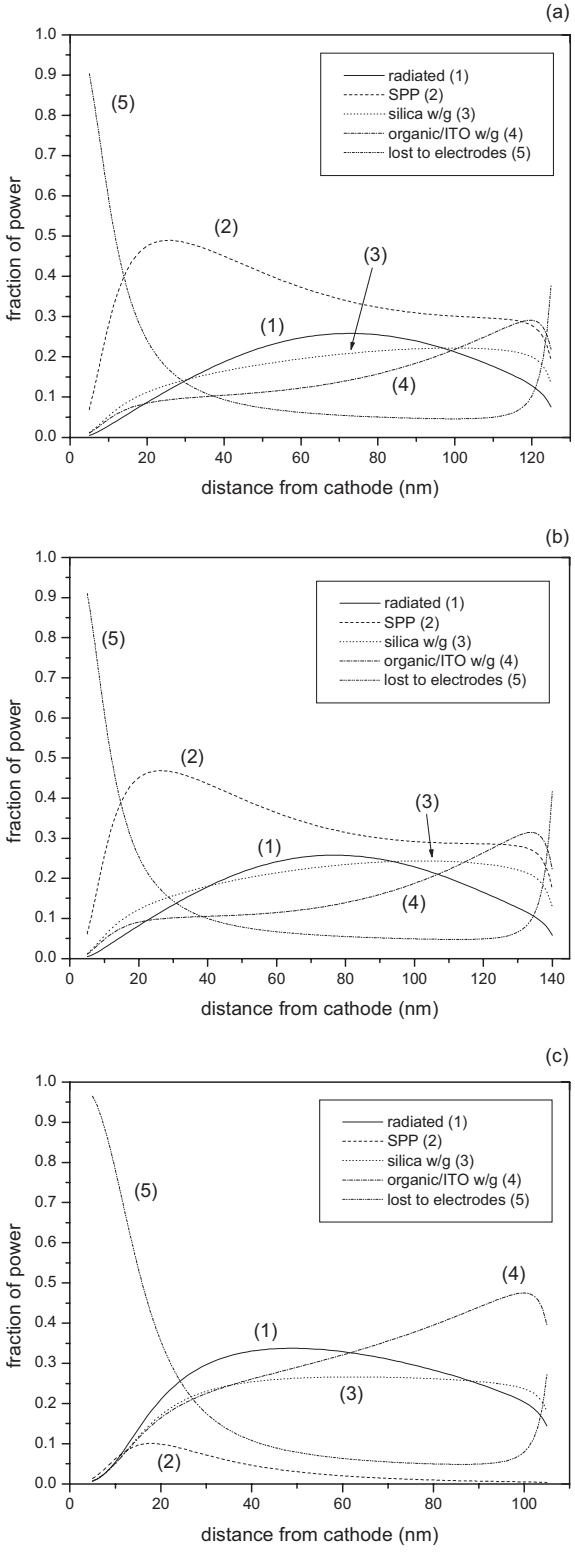

Figure 3. Fractional power plots for a) dendrimer, b) Alq_3, and c) MEH–PPV emissive layers. The PLQY is taken to be 1 (i.e., 100%) in all cases. w/g denotes waveguide modes.

to each mode. It is instructive to calculate these power fractions for a range of emitter positions within the emissive layer. Such a plot for the dendrimer structure is shown in Figure 3a.

3. Results

From Figure 3a, we can see that the optimum emitter position for the dendrimer-based OLED is with the emitters situated 73 nm from the Al cathode. For emitters at this position, 25.8 % of the total power is radiated from the structure—this figure is the optical out-coupling efficiency. The largest fraction of the power, 33.7 %, is lost to the SPP mode, with a small amount of power (5.3 %) lost to non-radiative absorption, being dissipated as heat within the electrical contacts. Loss of power to waveguide modes is split into two categories; loss to modes associated with the organic and ITO layers, 14.3 %, and loss to modes within the thick silica substrate, 20.9 %.

Figure 3b shows a similar fractional power plot for the Alq_3-based system. The maximum radiated power in this case is also 25.8 %. The similarity between the dendrimer and Alq_3 systems is due to both systems having effectively isotropic dipole moments and similar refractive indices. We again see significant coupling to the SPP mode, this being 32.0 % at the point of maximum radiation. The power lost to the SPP mode peaks at 46.8 % when the emitters are located at about 25 nm from the cathode. Although coupling to the SPP mode increases as the distance between the emitter and the metal decreases, coupling to losses in the metal increases faster, leading to a maximum in the SPP coupling at a distance of ~25 nm as noted before.[27,29] In these structures, with effective isotropic dipole-moment distributions, coupling to the SPP dominates over coupling to waveguide modes.

Using a polymer (MEH-PPV) emissive layer leads to very different power-loss characteristics (Fig. 3c). The maximum amount of power that can be radiated is now 33.7 %, with the emitters situated 49 nm from the cathode. The main power-loss mechanism in this case is the waveguide modes; 28.8 % of the total power is lost to modes guided in the organic/ITO layers, and 26.3 % to silica modes, when the emitters are located in this position. The power lost to waveguide modes is higher than for the other materials because of the higher refractive index of the polymer. The loss to the SPP is much reduced, this reduced coupling being due to the fact that the SPP mode is predominantly TM (transverse magnetic) polarized; the emissive dipole moments in the polymer lie in the plane of the layer and are thus poorly matched to the SPP field. The very different behavior of the conjugated polymer system compared to that of the dendrimer and Alq_3 systems arises primarily from the different orientation of the dipole moments in the two systems.

So far we have only discussed results where the PLQY has been assumed to be 1. We next consider what happens when this condition is relaxed, thus allowing us to take account of the measured PLQYs. We have taken a value of 0.78 for the dendrimer:CBP blend,[5] 0.32 for the Alq_3,[30] and 0.15 for the MEH–PPV.[31] We have chosen MEH–PPV because it is a well-known and well-characterized polymer. Some conjugated polymers have higher PLQY values, and the effect of this can be seen in Figure 4. Values for all three materials are still undergoing improvements, with industry indicating figures of between 0.40 and 0.70 for a variety of emissive polymers. Figure 5 shows plots for each of the three systems using these PLQY values. As expected, reducing the PLQY leads to an increased non-radiative loss and a scaling down of the efficiency of the radiative decay routes, including radiation, waveguide modes, and SPP modes.

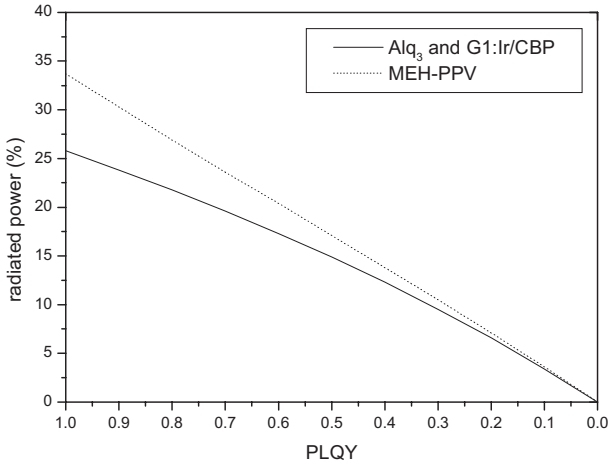

Figure 4. Plot showing the maximum possible out-coupling efficiency from a structure as a function of PLQY. The results for the Alq_3- and the dendrimer-based systems are almost identical and are represented by the same line.

Using the measured PLQY values for the three emissive systems, we see a significant drop in the percentage of power that can be radiated. Due to its relatively high PLQY value (0.78) the dendrimer system (Fig. 5a) proves the most efficient of the three systems, with the possibility of 21.4 % of the total power being radiated.

As expected, the power-loss characteristics for the Alq_3-based structure (Fig. 5b) offer a striking example of the importance of accounting for the quantum efficiency. Whereas, with a PLQY value of 1, this system and that based upon a dendrimer emissive layer had very similar characteristics, by changing the PLQY to the measured values the out-coupling efficiencies are seen to be very different. With a PLQY value of 0.32, the Alq_3-based system only radiates 10.1 % of the total power. It is a similar story for the MEH–PPV system (Fig. 5c). Again, the relatively low PLQY value of 0.15 means that the maximum amount of the total power that can be radiated is 5.2 %.

Figure 4 shows a plot of the maximum percentage of the total power that emerges as radiation (the out-coupling efficiency) as a function of PLQY for the three material systems. There are two features which are particularly worthy of note. The first concerns the shape of the curves. The relationship between radiation and PLQY is not linear. This highlights the importance of microcavity effects; one cannot simply take the maximum expected radiation (when PLQY = 1) and scale it by the relevant PLQY value. The second point is that the results for dendrimer- and Alq_3-based structures are almost identical

ADVANCED FUNCTIONAL MATERIALS

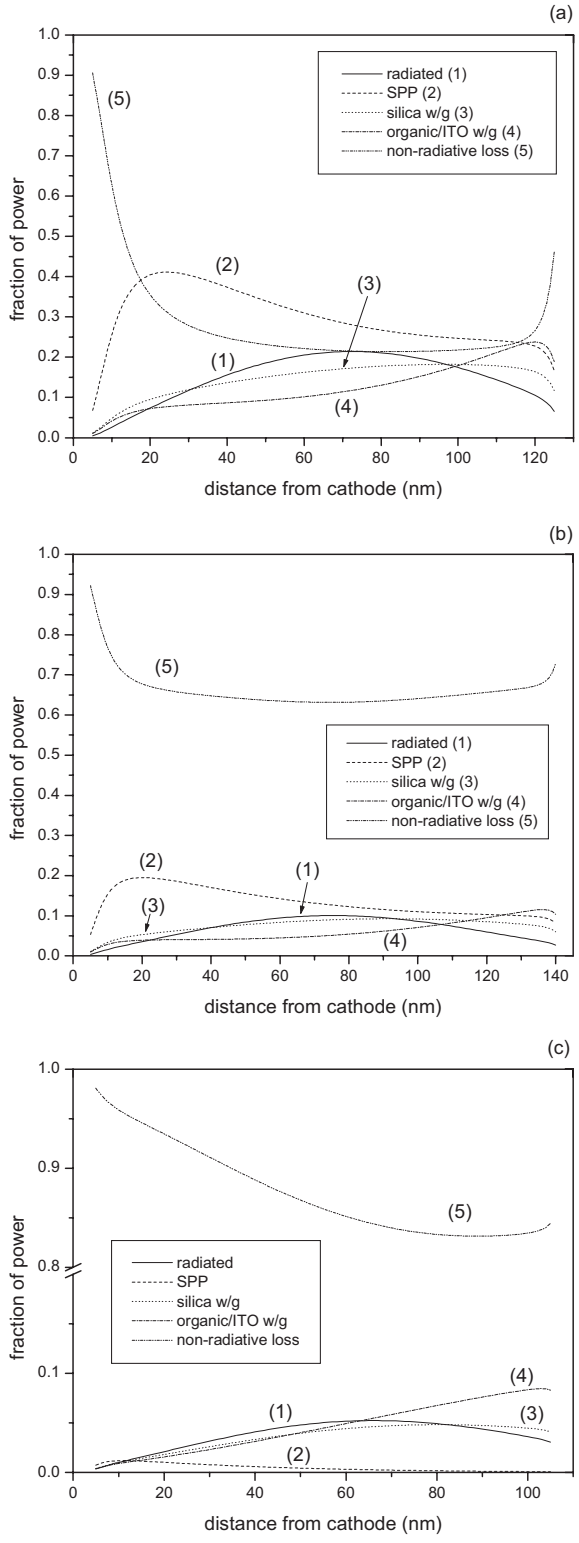

Figure 5. Fractional power plots for a) dendrimer, b) Alq_3, and c) MEH–PPV emissive layers. The PLQYs are taken to be 0.78, 0.32, and 0.15, respectively.

and are indistinguishable on the scale of this plot. This is due to the similar optical properties of these materials and the optimization of the organic-layer thicknesses.

4. Conclusions

We have seen that, when the PLQY is set to unity, the MEH–PPV system is the most efficient, with 33.7 % of the total power radiated. This compares with 25.8 % for the Alq_3- and dendrimer-based structures. The loss of power to other channels depends greatly on the dipole orientation of the emissive material in question, with waveguide modes dominating in the polymer case, and the SPP mode being dominant in the small-molecule and dendrimer systems. Importantly, we have demonstrated the dependence of the system efficiency on the value of the quantum efficiency. By using measured PLQY values for the various emissive layers, we have shown that the dendrimer-based structure is the most efficient. This is in large part due to the high PLQY of the dendrimer material. If one could also gain control over the orientation of the dipole moments in this material and place them in the plane of the device, even further increases in out-coupling efficiency should be possible. As noted above, a compromise may have to be reached between optical out-coupling optimization and electrical efficiency—this will be an important area for future study.

Appendix

Refractive indices of materials modeled:

We have assumed the silica substrates to be dispersionless, having a refractive index of 1.46. For the other materials, we included the effect of dispersion and chose to represent their refractive indices by polynomials.

1) Aluminum:

$$n = 19.92812 - 84.7052x + 140.1731x^2 - 111.85238x^3 + 43.46728x^4 - 653\,696x^5$$

$$k = 319.47025 - 1347.04872x + 2350.75746x^2 - 2149.03408x^3 + 1088.8157x^4 - 289.65148x^5 + 31.56516x^6$$

where n and k are the real and imaginary parts of the index, respectively, and x = wavelength (nm)/400.

2) ITO:

$$n = 1.67567 + 0.20122x$$

$$k = 0.005$$

with x = 1000/wavelength (nm).

3) Dendrimer:CBP blend:

$$n = 5.0939 - 7.72676x + 6.79507x^2 - 2.68704x^3 + 0.399x^4$$

with x = wavelength (nm)/400.

4) Alq_3:

$$n = -1.33075 + 8.69156x - 8.42617x^2 + 3.38293x^3 - 0.48725x^4$$

with x = wavelength (nm)/400.

5) MEH–PPV:

$$n_{\text{horizontal}} = 79.92516 - 225.33696x + 224.7041x^2 - 118.59501x^3 + 21.6389x^4$$

$$n_{\text{perpendicular}} = -5883.62922 + 28044.72196x - 55\,510.71725x^2 + 58\,431.97694x^3 - 34\,505.20622x^4 + 10\,840.0656x^5 - 1415.62534x^6$$

for values in and normal to the plane, with x = wavelength (nm)/550.

Received: May 9, 2005
Final version: June 8, 2005

[1] C. W. Tang, S. A. VanSlyke, *Appl. Phys. Lett.* **1987**, *51*, 913.
[2] J. H. Burroughes, D. D. C. Bradley, A. R. Brown, R. N. Marks, K. Mackay, R. H. Friend, P. C. Burn, A. B. Holmes, *Nature* **1990**, *347*, 539.
[3] M. A. Baldo, M. E. Thompson, S. R. Forrest, *Pure Appl. Chem.* **1999**, *71*, 2095.

[4] P. W. Wang, Y. J. Lui, C. Deradoss, P. Bharathi, J. S. Moore, *Adv. Mater.* **1996**, *8*, 237.
[5] T. D. Anthopoulos, J. P. J. Markham, E. B. Namdas, J. R. Lawrence, I. D. W. Samuel, S.-C. Lo, P. L. Burn, *Org. Electron.* **2003**, *4*, 71.
[6] T. D. Anthopoulos, J. P. J. Markham, E. B. Namdas, I. D. W. Samuel, S.-C. Lo, P. L. Burn, *Appl. Phys. Lett.* **2003**, *82*, 4824.
[7] J. A. E. Wasey, W. L. Barnes, *J. Mod. Opt.* **2000**, *47*, 725.
[8] W. L. Barnes, *J. Mod. Opt.* **1998**, *45*, 661.
[9] V. Bulovic, V. B. Khalfin, G. Gu, P. E. Burrows, D. Z. Garbuzov, S. R. Forrest, *Phys. Rev. B* **1998**, *58*, 3730.
[10] L. H. Smith, J. A. E. Wasey, W. L. Barnes, *Appl. Phys. Lett.* **2004**, *84*, 2986.
[11] J. M. Ziebarth, M. D. McGehee, *J. Appl. Phys.* **2005**, *97*, 064 502.
[12] P. A. Hobson, J. A. E. Wasey, I. Sage, W. L. Barnes, *IEEE J. Sel. Top. Quantum Electron.* **2002**, *8*, 378.
[13] J. M. Lupton, J. Matterson, I. D. W. Samuel, M. J. Jory, W. L. Barnes, *Appl. Phys. Lett.* **2000**, *77*, 3340.
[14] P. T. Worthing, W. L. Barnes, *Appl. Phys. Lett.* **2001**, *79*, 3035.
[15] I. Schnitzer, E. Yablonovitch, C. Caneau, T. J. Gmitter, A Scherer, *Appl. Phys. Lett.* **1993**, *63*, 2174.
[16] T. Yamasaki, K. Sumioka, T. Tsutsui, *Appl. Phys. Lett.* **2000**, *76*, 1243.
[17] C. F. Madigan, M.-H. Lu, J. C. Sturm, *Appl. Phys. Lett.* **2000**, *76*, 1650.
[18] T. Tsutsui, M. Yahiro, H. Yokogawa, K. Kawano, M.Yokoyama, *Adv. Mater.* **2001**, *13*, 1149.
[19] E. Buleier, W. Wehner, F. Vogtle, *Synthesis* **1978**, 155.
[20] D. A. Tomalia, H. Baker, J. R. Dewald, M. Hall, G. Kallos, S. Martin, J. Roeck, J. Ryder, P. Smith, *Polym. J.* **1985**, *17*, 117.
[21] S. Hecht, J. M. J. Frechet, *Angew. Chem. Int. Ed.* **2001**, *40*, 74.
[22] S.-C. Lo, N. A. H. Male, J. P. J. Markham, S. W. Magennis, P. L. Burn, O. V. Salata, I. D. W. Samuel, *Adv. Mater.* **2002**, *14*, 975.
[23] I. D. W. Samuel, *Philos. Trans. R. Soc. London, Ser. A* **2000**, *358*, 193.
[24] L. S. Hung, R. Q. Zhang, P. He, G. Mason, *J. Phys. D* **2002**, *35*, 103.
[25] C. W. Tang, S. A. VanSlyke, C. H. Chen, *J. Appl. Phys.* **1989**, *65*, 3610.
[26] H. Becker, S. E. Burns, R. H. Friend, *Phys. Rev. B* **1997**, *56*, 1893.
[27] G. W. Ford, W. H. Weber, *Phys. Rep.* **1984**, *113*, 195.
[28] H. Raether, *Surface Plasmons*, 1st ed., Springer, Berlin **1988**, Ch. 2, p. 4.
[29] I. Pockrand, A. Brilliante, D. Mobius, *Chem. Phys. Lett.* **1980**, *69*, 499.
[30] D. Z. Garbuzov, V. Bulovic, P. E. Burrows, S. R. Forrest, *Chem. Phys. Lett.* **1996**, *249*, 433.
[31] N. C. Greenham, I. D. W. Samuel, G. R. Hayes, R. T. Phillips, Y. A. R. R. Kessener, S. C. Moratti, A. B. Holmes, R. H. Friend, *Chem. Phys. Lett.* **1995**, *241*, 89.

FULL PAPERS

Organic LEDs

L. H. Smith, J. A. E. Wasey,
I. D. W. Samuel,
W. L. Barnes* ..... ■ – ■

Light Out-Coupling Efficiencies of Organic Light-Emitting Diode Structures and the Effect of Photoluminescence Quantum Yield

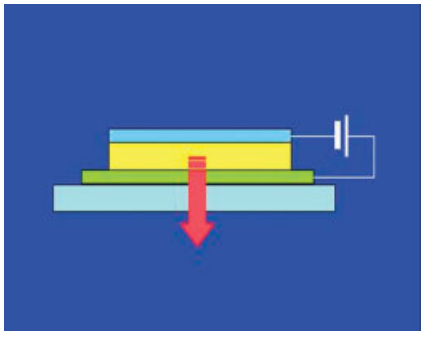

Light out-coupling efficiency is an important parameter that needs to be optimized for the full exploitation of organic light emitting diodes (OLEDs; see Figure). OLED designs optimized for light out-coupling for three different light-emitting material systems are theoretically investigated, and the effect of photoluminescence quantum yield is examined.

